Biochemical and Biophysical Research Communications 446 (2014) 375–379

Contents lists available at ScienceDirect

Biochemical and Biophysical Research Communications

journal homepage: www.elsevier.com/locate/ybbrc

An AFM-based pit-measuring method for indirect measurements of cell-surface membrane vesicles

Xiaojun Zhang [a,b], Yuan Chen [a], Yong Chen [a,b,*]

[a] Nanoscale Science and Technology Laboratory, Institute for Advanced Study, Nanchang University, Nanchang, Jiangxi 330031, China
[b] Department of Biotechnology, Nanchang University, Nanchang, Jiangxi 330031, China

ARTICLE INFO

Article history:
Received 20 February 2014
Available online 4 March 2014

Keywords:
Membrane vesicles
Vesicle-derived pits
Endothelial cells
Atomic force microscopy (AFM)

ABSTRACT

Circulating membrane vesicles, which are shed from many cell types, have multiple functions and have been correlated with many diseases. Although circulating membrane vesicles have been extensively characterized, the status of cell-surface membrane vesicles prior to their release is less understood due to the lack of effective measurement methods. Recently, as a powerful, micro- or nano-scale imaging tool, atomic force microscopy (AFM) has been applied in measuring circulating membrane vesicles. However, it seems very difficult for AFM to directly image/identify and measure cell-bound membrane vesicles due to the similarity of surface morphology between membrane vesicles and cell surfaces. Therefore, until now no AFM studies on cell-surface membrane vesicles have been reported. In this study, we found that air drying can induce the transformation of most cell-surface membrane vesicles into pits that are more readily detectable by AFM. Based on this, we developed an AFM-based pit-measuring method and, for the first time, used AFM to indirectly measure cell-surface membrane vesicles on cultured endothelial cells. Using this approach, we observed and quantitatively measured at least two populations of cell-surface membrane vesicles, a nanoscale population (<500 nm in diameter peaking at ~250 nm) and a microscale population (from 500 nm to ~2 μm peaking at ~0.8 μm), whereas confocal microscopy only detected the microscale population. The AFM-based pit-measuring method is potentially useful for studying cell-surface membrane vesicles and for investigating the mechanisms of membrane vesicle formation/release.

1. Introduction

Although the shedding of submicron membrane vesicles from the plasma membrane of cells was reported 40 years ago, initially as the release of "cell dust" and subsequently as "microparticles" [1], the multifaceted roles of [2] and mechanisms underlying [3] shed membrane vesicles or circulating microparticles have been intensively studied in the past decade. Membrane vesicles or circulating microparticles shed from activated or apoptotic cells play important roles in cell-to-cell communication [4,5], coagulation, inflammation, thrombosis, angiogenesis [6,7], cellular transplantation or solid graft [8], and many diseases [9,10].

Because membrane vesicles must be shed into the blood and circulate in the vasculature to exert specific functions, they have been characterized by different approaches including flow cytometry, antibody capture-based ELISA, electron microscopy, confocal microscopy, high performance liquid chromatography, capillary electrophoresis, mass spectrometry, and others [11]. In contrast, cell-surface membrane vesicles are less characterized and poorly measured quantitatively.

Among imaging tools, scanning electron microscopy and transmission electron microscopy have usually been utilized to characterize circulating or cell-surface membrane vesicles [12,13]. Atomic force microscopy (AFM) is a powerful tool for surface imaging that has been successfully used for in situ observation of cell-surface ultrastructures at the nanoscale in liquid or air [13–15]. Since its recent introduction as a tool to detect circulating membrane vesicles [16,17], AFM has increasingly been used to image substrate-deposited plasma membrane vesicles [18,19]. However, to the best of our knowledge, there has been no report about AFM detection of cell-surface membrane vesicles on eukaryotic cells until now.

Unfortunately, direct AFM imaging and measurement of cell surface membrane vesicles proved to be very difficult due to the similarity of surface morphology between membrane vesicles and cell surfaces. Here, we developed an AFM-based pit-measuring method to indirectly measure cell-bound membrane vesicles by imaging and measuring the membrane vesicle-derived pits using AFM.

* Corresponding author at: 999 Xuefu Ave., Honggutan District, Nanchang, Jiangxi 330031, China. Fax: +86 791 83969963.
E-mail address: dr_yongchen@hotmail.com (Y. Chen).

http://dx.doi.org/10.1016/j.bbrc.2014.02.114
0006-291X/

2. Materials and methods

2.1. Cells and cell culture

Human umbilical vein endothelial cells (HUVECs) purchased from Xiangya Central Experiment Laboratory (Hunan, China) were cultured in Dulbecco's modified Eagle's medium (DMEM) (Gibco) supplemented with 10% (w/v) fetal calf serum (Hyclone, South Logan, UT), 100 U/ml penicillin, and 100 μg/ml streptomycin. For all experiments, cell cultures were passaged approximately five times.

2.2. Dynamic observation of vesicle-pit transformation by confocal microscopy

The procedure for sample preparation and dynamic observation was performed as previously described [20]. Approximately 2×10^4/ml HUVECs were cultured in a petri dish for 24 h in a CO_2 incubator (37 °C, 5% CO_2). The cells were then washed twice with PBS and fixed with 4% paraformaldehyde in PBS for 30 min. Then, after washing the cells once with PBS and twice with distilled water, the petri dish was mounted on the stage of an LSM710 confocal microscope (Carl Zeiss, Oberkochen, Germany). After taking an image of the cells the liquid in the petri dish was quickly sucked up, the sample air dried, and the cells in the same field imaged every 30 s for a period of 25 or 60 min. Although images were automatically taken every 30 s, only the images shown in the figures were processed and presented.

2.3. Atomic force microscopy

An Agilent series 5500 AFM (Agilent Technologies, CA) was used in our studies. The length, width, and thickness of the Si_3N_4 AFM cantilevers were 225, 38, and 7 μm, respectively, with a resonant frequency of 190 kHz and a force constant of 48 N/m. AFM imaging was performed in the tapping mode at a scan rate of 0.5 Hz in air. The cells were fixed with 4% paraformaldehyde in PBS for 30 min, washed once with PBS and twice with distilled water, air dried for 0.5–1 h, and subjected to AFM imaging in air. After an individual whole cell was imaged, multiple local areas on the cell were imaged again by AFM.

2.4. Data processing and statistical analysis

PicoView 1.12 equipped with Aligent series 5500 AFM was used to process the AFM images. All confocal data were processed using the Zeiss LSM710 Zen Software. The distribution histograms were made by EasyFit 5.5 (MathWave Technologies, Dnipropetrovsk, Ukraine). All values are expressed as the mean ± SD (Three independent experiments were performed). Statistical analyses were performed using Student's t test. $P < 0.05$ was considered statistically significant.

3. Results

3.1. Visualization of the dynamic, air-drying-induced transformation of membrane vesicles on prefixed HUVECs into pits using confocal microscopy

Interestingly, we found that air drying the fixed cells resulted in the transformation of most membrane vesicles into plasma membrane pits with sizes similar to that of the vesicles. To verify this observation, we monitored the process in real-time using confocal microscopy. Fully spread HUVECs in a petri dish were prefixed in 4% paraformaldehyde for 30 min, followed by one wash with PBS and two washes with distilled water. Next, the petri dish with the fixed cells in distilled water was mounted onto the stage of a confocal microscope. After the water in the petri dish was sucked up, the dynamic process of the membrane vesicles transforming into pits was imaged during air drying at room temperature for the indicated amount of time (Fig. 1).

Fig. 1A shows the morphological changes of membrane vesicles on three cells at six indicated time points during air drying for 25 min. At the first four time points, the gradual evaporation of water from the cell surfaces was evident. After air drying for 9 min, many membrane vesicles on the three cells changed into pits within seconds, and approximately 25 min later, most of the membrane vesicles had transformed into pits. The higher-magnification images in Fig. 1B show that the majority of membrane vesicles in the local region of a cell were transformed into pits after air drying the cells for 60 min.

Most importantly, after air drying for 30–60 min, most of the pits appeared exactly at the position of each corresponding membrane vesicle on the cell surface. Some pits also appeared at places where membrane vesicles were absent in the confocal images. It is possible that these pits were derived from small membrane vesicles that were undetectable or unidentified by confocal microscopy due to the relatively weak phase contrast. In general, although most pits formed immediately (within seconds) after evaporation of the water covering the vesicle some membrane vesicles might take different periods of time to transform into pits due to different evaporation speeds of the vesicle-covering water. In our study, air drying for a period of 30–60 min was sufficient to trigger the transformation of most membrane vesicles into pits. To ensure the transformation of as many membrane vesicles as possible into pits, we dried the samples for approximately 1 h for the AFM imaging experiment described below.

3.2. AFM imaging of the membrane vesicle-derived pits on dried prefixed cells

To test the efficacy of this pit-measuring method (i.e., measuring vesicle-derived pits instead of membrane vesicles themselves), we utilized AFM in the tapping mode to image the prefixed dried resting HUVECs in air (Fig. 2). After a single cell (Fig. 2A) was imaged by AFM, multiple local regions (10 μm × 10 μm) on the cell were imaged again at a higher magnification (Fig. 2B–E). Many relatively large membrane vesicle-derived pits (~1 micron in diameter) were already evident in the low-magnification AFM image of the whole cell (Fig. 2A). At higher magnifications (Fig. 2B–E), many small pits (a few hundreds nanometers in diameter) were clearly visible in the AFM topographical images. The cross-section height profiles in Fig. 2F and G show the relatively large pits indicated by arrows and the small pits indicated by arrowheads.

3.3. Size distributions of membrane vesicles and the vesicle-derived pits on cells visualized by confocal microscopy and AFM, respectively

Next, we quantified membrane-vesicles and vesicle-derived pits of various sizes based on the confocal and AFM topographical images. Because the small membrane vesicles were undetectable or hardly measurable in the confocal DIC images, only one peak was observed in the confocal-based size distribution of membrane vesicles on HUVECs measure in liquid, and this peak averaged 0.963 ± 0.147 μm in diameter (Fig. 3A). Whereas the AFM-based size distribution of vesicle-derived pits on air-dried HUVECs displayed two peaks, one ranging from 100 nm to 500 nm and peaking at approximately 250 nm and the other one ranging from 500 nm to 1.5 μm and peaking at approximately 0.8 μm. Overall, the pit size measured from the AFM images averaged 0.523 ± 0.314 μm (Fig. 3B).

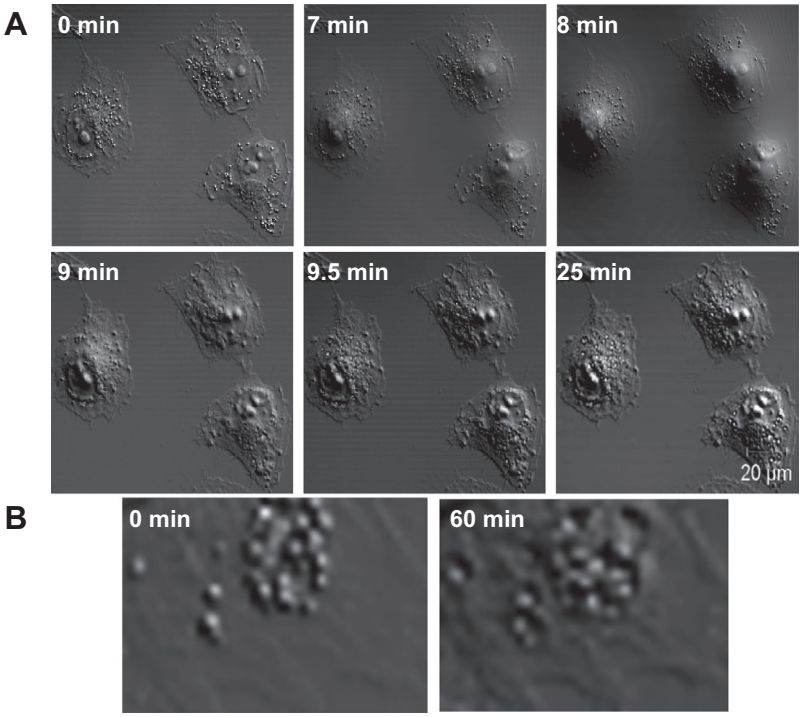

Fig. 1. The dynamic process of the air drying-induced transformation of most membrane vesicles into pits in the plasma membrane of prefixed HUVECs was visualized by confocal microscopy. (A) Confocal DIC images showing the morphological changes of membrane vesicles on three cells at six indicated time points during air drying for a period of 25 min. At the first four time points, the gradual evaporation of water from the cell surfaces is evident. After air drying for 9 min, many membrane vesicles on the three cells changed into pits within seconds, and after 16 min of more air drying, most membrane vesicles transformed into pits. (B) Higher-magnification confocal DIC images showing the transformation of most membrane vesicles in a local region of a cell into pits after air drying for 60 min (right image). Scale bar: 20 μm.

4. Discussion

Given its great success in imaging cell-surface ultrastructures in many cell types [13,21,22], AFM has the potential to be an ideal tool for imaging membrane vesicles on cell surfaces. In practice, however, the difficulties in obtaining high quality images of cell-surface membrane vesicles and/or distinguishing the membrane vesicles from the wavy cell surface in AFM topographical images are major obstacles to the direct measurement of membrane vesicles on cells in liquid. The topography of local cell surfaces imaged by AFM is generally in a wavy shape. Therefore, it is difficult to determine whether an AFM-detected small projection is a membrane vesicle. Moreover, relatively large membrane vesicles on a cell are very easy to be deformed due to the pressure of the AFM tip during imaging in liquid especially using the contact mode which also causes membrane vesicles undistinguishable. These obstacles might be the reason why no studies on direct AFM imaging of cell-bound membrane vesicles have been reported until now.

Interestingly, we found that air drying was able to transform most cell-surface membrane vesicles into pits of similar size in the plasma membrane (Fig. 1) and that the strong contrast between pits and the cell surface made the pits easily distinguishable in an AFM topographical image (Fig. 2). These observations support the use of AFM-mediated detection of vesicle-derived pits as an indirect method for measuring cell-surface membrane vesicles. AFM could observe many small pits (Fig. 2B–E) potentially derived from small membrane vesicles which were undetectable by confocal microscope (Fig. 1). The comparison of the size distribution of AFM-detectable, vesicle-derived pits with that of confocal microscopy-detectable membrane vesicles on cells (Fig. 3) further supports the sensitivity and accuracy of the AFM-based, pit-measuring method. This novel approach was able to detect membrane vesicles on the nanoscale range with a double-peaked size distribution ranging from 100 nm to 1500 nm in diameter (Figs. 2 and 3). In contrast, phase contrast confocal microscopy was only able to detect vesicles on the microscale range, with a single-peak size distribution ranging from approximately 500 nm to 1500 nm (Figs. 1 and 3A).

Based on AFM data, HUVECs most likely exist in at least two populations of cell-surface membrane vesicles, with different sizes. The population on the nanoscale range has a diameter of approximately 100–500 nm and the other population is of the microscale size (>500 nm). There potentially exists another population of cell-surface membrane vesicles with a diameter of less than 100 nm, such as the membrane-bound precursors of the so-called "exosomes" [23]. Unfortunately, this AFM-based, pit-measuring method is currently unable to detect these tiny structures due to some unknown reasons. For example, the structures are too tiny to be torn apart by the water-evaporation-induced driven force to transform into pits, or even if they transform into pits, the pits are too tiny to be distinguished from the wavy cell surface in AFM topographical images.

This AFM-based, pit-measuring method has some limitations. Firstly, it is hard to detect tiny membrane vesicles of less than 100 nm as above mentioned. Secondly, this approach can not distinguish small vesicle-derived pits from preexisting membrane invaginations. However, most preexisting membrane invaginations, e.g., clathrin-coated pits and caveolae (a type of lipid/membrane raft), generally have a size of approximately or even less than 100 nm [24,25]. Therefore, the combination of the two limitations makes AFM measurement of membrane vesicles of less than 100 nm more challenging. More in-depth studies will be needed to address this problem. Thirdly, this method cannot monitor the dynamic changes of cell-surface membrane vesicles since the transformation of the vesicles into pits has to be performed prior to AFM imaging. However, compared with electron microscopy which is also hard to observe the dynamic changes of membrane

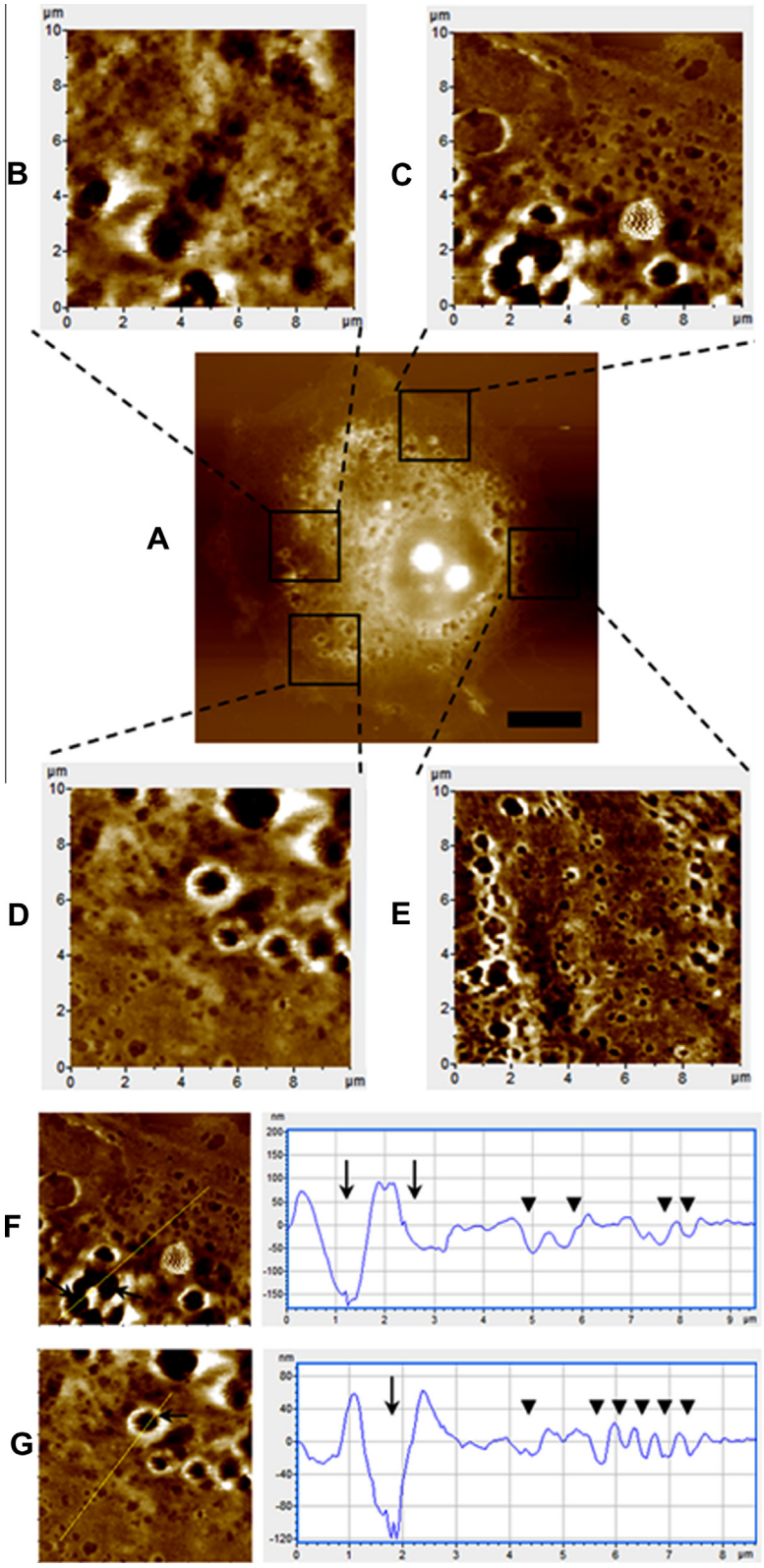

Fig. 2. AFM images of the membrane vesicle-derived pits on prefixed dried HUVECs in air. (A) AFM topographical image of a single cell. Scale bar: 10 μm. (B-E) AFM topographical images of four local regions on the cell indicated by the corresponding squares in Fig. 2A. (F, G) Height profiles (right) of the cross sections across the lines in the topographical images (left). The arrows and arrowheads indicate the large (~1 μm in diameter) and small (a few hundreds nanometers) pits, respectively.

vesicles, the sample preparation procedure for our method is much simpler and label-free.

Despite these limitations, the AFM-based pit-measuring method is potentially a useful, simple but effective approach for studying cell-surface membrane vesicles. For the first time, AFM was used in this study to measure cell-surface membrane vesicles although indirectly. This approach may be an important development in technique for measuring cell-surface membrane vesicles. It is a good start and may open a new window for revealing the mechanisms of membrane vesicle formation/release in the future.

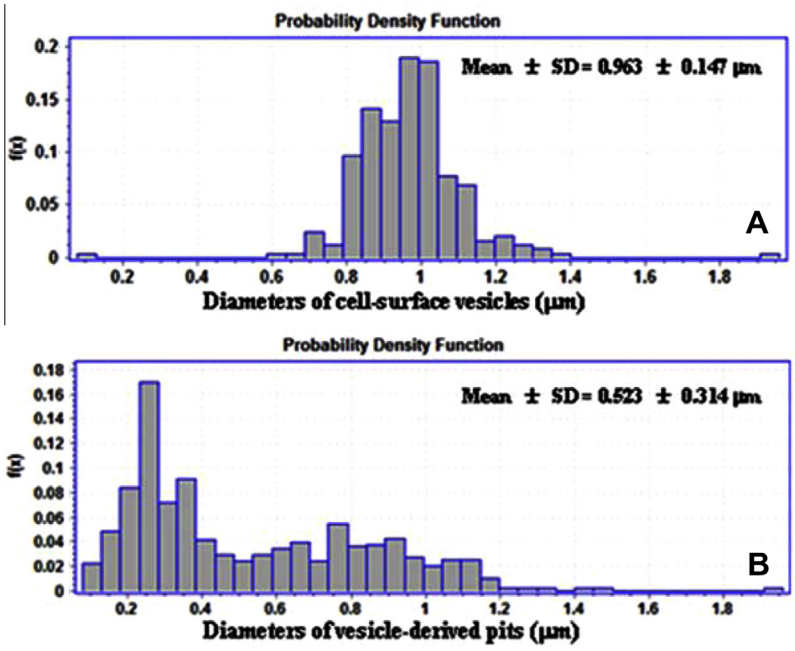

Fig. 3. Size distributions in diameter of membrane vesicles or vesicle-derived pits on HUVECs. (A) Confocal microscopy-based size distribution of membrane vesicles on five prefixed HUVECs in liquid shows only one population of vesicles with a microscale diameter peaking at ~1 μm. (B) AFM-based size distribution of vesicle-derived pits on six prefixed dried HUVECs displays two populations of vesicles, the microscale one peaking at ~0.8 μm and a nanoscale population peaking at ~250 nm.

Acknowledgments

This study was supported by the National Natural Science Foundation of China (31260205) and the Scientific Research Foundation for Returned Overseas Chinese Scholar of State Education Ministry.

References

[1] C.M. Boulanger, F. Dignat-George, Microparticles: an introduction, Arterioscler. Thromb. Vasc. Biol 31 (2011) 2–3.
[2] F. Dignat-George, C.M. Boulanger, The many faces of endothelial microparticles, Arterioscler. Thromb. Vasc. Biol 31 (2011) 27–33.
[3] O. Morel, L. Jesel, J.M. Freyssinet, F. Toti, Cellular mechanisms underlying the formation of circulating microparticles, Arterioscler. Thromb. Vasc. Biol 31 (2011) 15–26.
[4] J. Ratajczak, M. Wysoczynski, F. Hayek, A. Janowska-Wieczorek, M.Z. Ratajczak, Membrane-derived microvesicles: important and underappreciated mediators of cell-to-cell communication, Leukemia 20 (2006) 1487–1495.
[5] S. Tual-Chalot, D. Leonetti, R. Andriantsitohaina, M.C. Martinez, Microvesicles: intercellular vectors of biological messages, Mol. Interv 11 (2011) 88–94.
[6] O. Morel, N. Morel, L. Jesel, J.M. Freyssinet, F. Toti, Microparticles: a critical component in the nexus between inflammation, immunity, and thrombosis, Semin. Immunopathol 33 (2011) 469–486.
[7] A.S. Leroyer, F. Anfosso, R. Lacroix, F. Sabatier, S. Simoncini, S.M. Njock, N. Jourde, P. Brunet, L. Camoin-Jau, J. Sampol, F. Dignat-George, Endothelial-derived microparticles: Biological conveyors at the crossroad of inflammation, thrombosis and angiogenesis, Thromb. Haemost 104 (2010) 456–463.
[8] B. Bakouboula, O. Morel, A.L. Faller, J.M. Freyssinet, F. Toti, Significance of membrane microparticles in solid graft and cellular transplantation, Front. Biosci 16 (2011) 2499–2514.
[9] G.N. Chironi, C.M. Boulanger, A. Simon, F. Dignat-George, J.M. Freyssinet, A. Tedgui, Endothelial microparticles in diseases, Cell. Tissue. Res 335 (2009) 143–151.
[10] M.C. Martinez, S. Tual-Chalot, D. Leonetti, R. Andriantsitohaina, Microparticles: targets and tools in cardiovascular disease, Trends. Pharmacol. Sci 32 (2011) 659–665.
[11] A.S. Shet, Characterizing blood microparticles: technical aspects and challenges, Vasc. Health. Risk. Manag 4 (2008) 769–774.
[12] V. Combes, A.C. Simon, G.E. Grau, D. Arnoux, L. Camoin, F. Sabatier, M. Mutin, M. Sanmarco, J. Sampol, F. Dignat-George, In vitro generation of endothelial microparticles and possible prothrombotic activity in patients with lupus anticoagulant, J. Clin. Invest 104 (1999) 93–102.
[13] D.J. Muller, Y.F. Dufrene, Atomic force microscopy: a nanoscopic window on the cell surface, Trends. Cell. Biol 21 (2011) 461–469.
[14] I. Casuso, F. Rico, S. Scheuring, Biological AFM: where we come from–where we are–where we may go, J. Mol. Recognit 24 (2011) 406–413.
[15] X. Shi, X. Zhang, T. Xia, X. Fang, Living cell study at the single-molecule and single-cell levels by atomic force microscopy, Nanomedicine (Lond) 7 (2012) 1625–1637.
[16] Y. Yuana, T.H. Oosterkamp, S. Bahatyrova, B. Ashcroft, P. Garcia, Atomic force microscopy: a novel approach to the detection of nanosized blood microparticles, J. Thromb. Haemost 8 (2010) 315–323.
[17] J.M. Freyssinet, F. Toti, Membrane microparticle determination: at least seeing what's being sized!, J Thromb. Haemost 8 (2010) 311–314.
[18] H.S. Leong, T.J. Podor, B. Manocha, J.D. Lewis, Validation of flow cytometric detection of platelet microparticles and liposomes by atomic force microscopy, J. Thromb. Haemost 9 (2011) 2466–2476.
[19] B.A. Ashcroft, J. de Sonneville, Y. Yuana, S. Osanto, R. Bertina, M.E. Kuil, T.H. Oosterkamp, Determination of the size distribution of blood microparticles directly in plasma using atomic force microscopy and microfluidics, Biomed. Microdevices 14 (2012) 641–649.
[20] F. Zeng, W. Yang, J. Huang, Y. Chen, Y. Chen, Determination of the lowest concentrations of aldehyde fixatives for completely fixing various cellular structures by real-time imaging and quantification, Histochem. Cell. Biol 139 (2013) 735–749.
[21] D.J. Muller, AFM: a nanotool in membrane biology, Biochemistry 47 (2008) 7986–7998.
[22] L. Wu, J. Huang, X. Yu, X. Zhou, C. Gan, M. Li, Y. Chen, AFM of the ultrastructural and mechanical properties of lipid-raft-disrupted and/or cold-treated endothelial cells, J. Membr. Biol. 247 (2014) 189–200.
[23] B. Gyorgy, T.G. Szabo, M. Pasztoi, Z. Pal, P. Misjak, B. Aradi, V. Laszlo, E. Pallinger, E. Pap, A. Kittel, G. Nagy, A. Falus, E.I. Buzas, Membrane vesicles, current state-of-the-art: emerging role of extracellular vesicles, Cell. Mol. Life. Sci 68 (2011) 2667–2688.
[24] B. Ritter, S. Murphy, H. Dokainish, M. Girard, M.V. Gudheti, G. Kozlov, M. Halin, J. Philie, E.M. Jorgensen, K. Gehring, P.S. McPherson, NECAP 1 regulates AP-2 interactions to control vesicle size, number, and cargo during clathrin-mediated endocytosis, PLoS. Biol 11 (2013) e1001670.
[25] R.G. Parton, K. Simons, The multiple faces of caveolae, Nat. Rev. Mol. Cell. Biol 8 (2007) 185–194.